

Hydrodynamic performance evaluation of a tidal turbine with leading-edge tubercles

**Weichao Shi^{*1}, Roslyna Rosli¹, Mehmet Atlar¹, Rosemary Norman¹, Dazheng Wang²,
Wenxian Yang¹**

1 School of Marine Science and Technology, Newcastle University, UK

**2 School of Naval Architecture and Ocean Engineering, Harbin Institute of Technology,
Weihai, PR China**

Corresponding Author:

Weichao Shi, w.shi6@newcastle.ac.uk

**School of Marine Science and Technology
Armstrong Building, Newcastle University
United Kingdom, NE1 7RU
Tel: 0044 (0)191 222 6726
Fax: 0044 (0)191 222 5491**

Abstract: This paper contributes to the investigations into the feasibility of improving the performance of a marine current turbine using a biomimetic concept inspired from the leading-edge tubercles on the flippers of humpback whales. An experimental test campaign was recently conducted in the Emerson Cavitation Tunnel at Newcastle University and details of this test campaign together with the findings are summarised in the paper.

A set of tidal turbines with different leading-edge profiles was manufactured and tested to evaluate the hydrodynamic performance. Various tests were conducted at different flow speed and different pitch angle settings of the turbine blades. The results showed that the models with the leading-edge tubercles had higher power coefficients at lower tip speed ratios (TSRs) and at lower pitch angle settings where the turbine blades were working under stall conditions. Therefore, the tubercles can reduce the turbines' cut-in speed to improve the starting performance. The biomimetic concept did not compromise the maximum power coefficient value of the turbine, being comparable to the device without the tubercles, but shifted the distribution of the coefficient over the range of the tip speed ratios tested.

Keywords: Tidal turbine, Leading-edge tubercle, Model test, Hydrodynamic performance

1 Introduction

With the depletion of the traditional fossil energy sources, protection of energy reserves has been high on the agenda of many governments. Massive investment has been made in the renewable energy field to exploit sustainable energy resources. Tidal energy is a sustainable energy resource resulting from the gravitation effects of the sun and the moon, which has become a very attractive option as it is a significant resource which is highly predictable (Bahaj et al., 2007; Khan et al., 2009). However, the development of this technology for a given site is highly dependent on the local tidal current speeds and most areas around the world have rather moderate current speeds ranging from 1 to 2 m/s. To exploit tidal energy in such areas requires some improvement in the design of tidal energy devices to adapt to low flow speed conditions.

Recently the tubercles on the leading edges of humpback whale flippers have drawn the attention of researchers working in the field of tidal energy and wind energy, as these round protuberances along the leading edges have the ability to delay the stall and improve the lift-to-drag ratio of blades (Johari et al., 2007; K. L. Hansen et al., 2009; Miklosovic et al., 2007; Stanway, 2008; Weber et al., 2010; Yoon et al., 2011). Many research studies, which are both numerical and experimental in nature, have investigated the influence of the leading-edge tubercles as applied on air fans, wind turbines, rudders and so on (Corsini et al., 2013; Howle, Jan 24, 2009; Swanson and Isaac, 2011; van Nierop et al., 2008; Weber et al., 2010). According to these studies, blades with leading-edge tubercles can maintain lift coefficients further beyond the stall point in comparison to those without tubercles.

Based on these applications a study was made recently to improve a tidal turbine by applying tubercles to the blades and performance comparisons of tidal turbine models with different tubercle designs were carried out in a towing tank (Gruber et al., 2011). Even though some performance improvement was demonstrated in this testing, because the power coefficients were rather low compared with the other tidal turbines, the findings have been questioned on the grounds of whether the performance improvement was due to the effect of the leading-edge tubercles or whether it was accidental. Therefore, there is scope for further research to explore and validate this biomimetic concept via other turbine applications where the turbine models have better performances.

Within the above framework, this paper investigates the hydrodynamic performance of tidal turbines with and without leading-edge tubercles. A preliminary hydrofoil study was conducted to look at the effect of the leading-edge tubercles as applied to a “straightened” turbine blade which was based on a tidal turbine designed and tested in the Emerson Cavitation Tunnel (ECT) at Newcastle University (Shi et al., 2015). With the knowledge gained from this earlier hydrofoil study, three tidal turbines with different leading-edge profiles have been designed and tested in the ECT. In the remaining sections of the paper, the details of the turbine design and models, performance tests and results from the tests are presented and discussed to demonstrate the effect of the leading edge tubercles mainly on the torque, thrust, efficiency and cavitation performance.

2 Design and manufacture of the models

A horizontal axis tidal turbine (HATT) was chosen to be the reference turbine to which the leading-edge tubercles would be applied. This turbine model was designed and tested during a

previous project (Wang et al., 2007) and validated by a CFD study (Shi et al., 2013). The blade sections of the reference turbine were selected based on the NREL S814 foil section, as shown in Figure 1. The main particulars for the blades of this 400mm diameter model turbine are shown in Table 1.

The profile design of the leading edge tubercles was conducted in a previous study as reported in (Shi et al., 2015). In that study a “straightened” representative blade, which was designed based on the reference turbine blade with a constant pitch angle, was manufactured and tested for validations in the ECT, as shown in Figure 2. The smooth leading edge profile of the reference blade were replaced by two sets of leading edge tubercle profiles and compared. The reference turbine was assigned as “Ref” while the one with two leading-edge tubercles was named as “Sin2” and the one with eight leading-edge tubercles was named as “Sin8”. As shown in Figure 3, this study confirmed the significant benefits for the lift coefficients (C_L) caused by the leading-edge tubercles despite a slight increase in their drag coefficients (C_D). Furthermore, based on the lift-to-drag coefficient (C_L/C_D) performance, as shown in Figure 4, Sin2 displayed the best overall performance. This was largely due to the increased lift-to-drag coefficients over a wider range of angles of attack.

Based on the investigations in (Shi et al., 2015) three pitch adjustable turbine models with different leading-edge profiles were manufactured, as shown Figure 5. The turbine model with smooth leading edge (i.e. without tubercles) is named “Ref”; while the one with two leading-edge tubercles at the tip is named “Sin_2”; and the one with eight leading-edge tubercles is named “Sin_8”. The sinusoidal leading-edge profile was developed as shown in Figure 6. The amplitude (A) of the sinusoidal tubercles was equal to 10% of the local chord length (C) while eight tubercles were evenly distributed along the radius with the wavelength (W) equal to 20mm. The profile of the leading tubercles was as represented by Equation 1.

$$H = \frac{A}{2} \cos \left[\frac{2\pi}{W} (r - 40) - \pi \right] + \frac{A}{2} \quad \text{Equation 1}$$

Where H is the height of the leading-edge profile relative to the reference one which is the smooth leading-edge profile.

3 Experimental set-up

The three tidal turbine models were manufactured by Centrum Techniki Okrętowej S.A. (CTO, Gdansk) and tested in the Emerson Cavitation Tunnel at Newcastle University. The sketch of the tunnel is shown in Figure 7. The tunnel is a medium size propeller cavitation tunnel with a measuring section of 1219mm×806mm (width × height). The speed of the tunnel water varies between 0.5 and 8 m/s. Full details of the ECT can be found in (Atlar, 2011).

The turbine was mounted on a vertically driven dynamometer K&R H33, designed to measure the thrust and torque of a propeller or turbine. The main technical data of H33 is given in Table 2. A 64kW DC motor is mounted on top of the dynamometer to control the rotational speed of the turbine.

During the model test the torque and thrust of the turbine were measured and from these measurements the power coefficient and the thrust coefficient can be derived by using the following equations:

$$C_p = \frac{Q\omega}{\frac{1}{2}\rho A_T V^3} \quad \text{Equation 2}$$

$$C_T = \frac{T}{\frac{1}{2}\rho A_T V^2} \quad \text{Equation 3}$$

where Q is the torque of the turbine, Nm; T is the thrust, N; ω is the rotational speed, rad/s; A_T is the swept area of the turbine and equals to $\pi D^2/4$, m²; ρ is the tunnel water density, kg/m³; V is the incoming velocity, m/s, D is the turbine diameter, m.

The rotational speed is controlled by the motor to achieve the desired tip speed ratio (TSR) which can be calculated by Equation 4. As the performance of the turbine is strongly dependent on the Reynolds number and the cavitation number, these two non-dimensional numbers at 0.7 radius of the turbine blade, $Re_{0.7r}$ and $Cav_{0.7r}$ were monitored and can be derived from Equation 5 and Equation 6 respectively.

$$TSR = \frac{\omega r}{V} \quad \text{Equation 4}$$

$$Re_{0.7r} = \frac{C_{0.7r} \sqrt{(V^2 + (0.7\omega r)^2)}}{\nu} \quad \text{Equation 5}$$

$$Cav_{0.7r} = \frac{P_{0.7r} - P_v}{\frac{1}{2}\rho \sqrt{(V^2 + (0.7\omega r)^2)}} \quad \text{Equation 6}$$

where $C_{0.7r}$ is the chord length of the turbine at 0.7 radius, m; ν is the kinematic viscosity of the water, m²/s; $P_{0.7r}$ is the static pressure at the upper 0.7 radius of the turbine, Pa; P_v is the vapour pressure of the water, Pa.

During the tests, the incoming flow velocity of the tunnel was fixed and the rotational speed was varied to achieve a certain TSR required. The tests were conducted according to the test matrix shown in Table 3. The test conditions are also shown in graphical format in Figure 8. At high Reynolds numbers, due to the increased incoming velocity, cavitation number was reduced and hence cavitation might occur at the turbine blades. Taking advantage of the pitch adjustable design, three different pitch angles of the turbine blades were tested.

With this method, each condition was repeated three times for uncertainty analysis. The average results were then plotted and compared. The average standard deviation for C_p was around 2.9% and 0.7% for C_T . A sample of the uncertainty analysis is shown in Figure 9. As shown in the figure, the tests were quite repeatable.

4 Results

In order to analyse the effect of the leading-edge tubercles independently, each turbine model was tested by using the test matrix shown in Table 3. The performance was then compared for each test condition, for the reference turbine and the other two turbines with the tubercles. All of the cases were coded as “Model Name_Pitch Angle_Test Velocity”, for example “Ref_0_2” indicated the test results for the reference turbine model with 0° pitch angle setting tested at 2m/s incoming velocity.

4.1 Effect of Reynolds number and blade cavitation

As shown in Table 3 and Figure 8, the Reynolds number and cavitation number are cross-related to each other at constant tunnel pressure and are determined by the incoming velocity and TSRs. In order to study the influence of the Reynolds number and the cavitation number, the reference turbine model with the smooth leading edge was first tested under different incoming velocities, i.e. 2, 3 and 4 m/s while the blade pitch angle was set to 0°.

Based on the test results, the power coefficients, C_p , and thrust coefficients, $C_t/10$ were calculated and are presented in Figure 10. In this figure, the C_p curves marked in red are the data where cavitation inception occurred. The test results indicated that while the C_p curve would be greatly influenced by the blade cavitation, increasing the Reynolds number would only lead to a slight enhancement in the performance. However, this was also based on the types of cavitation developed.

During the tests, various types of cavitation were observed including tip vortex cavitation and cloud cavitation at the back-side and face-side of the blade, as shown in Figure 11, which depends on the TSR. The development sequence of these cavitation types on the blades was usually that the tip vortex cavitation first appeared and then gradually transformed to a more severe and unsteady cloud cavitation on either side of the turbine blade depending on the TSR. While the cloud cavitation would greatly reduce the turbine efficiency, it could also cause erosion on the blades.

Based on the test results it was noticed that Reynolds number and tip vortex cavitation had a limited influence on the turbine performance in comparison to the effect of the cloud cavitation which would not only cause efficiency loss but also was expected to cause erosion damage on the blades. It is therefore important to compare the turbine performance not only based on the same TSR but also based on the same Reynolds number as well as the cavitation number.

4.2 Effect of blade pitch angle

Another important factor that influences the turbine performance is the blade pitch angle. During the tests three different pitch angles, 0°, +4° and +8° were imposed on the turbine blades. From the test results of the reference turbine, as shown in Figure 12, the $C_t/10$ was significantly reduced by increasing the pitch angle. On the other hand, the C_p reached its maximum value (0.49), with +4° pitch angle, while +8° pitch angle provided the turbine with a better performance over the lower range of TSRs up to $TSR=2.5$.

Based on the test results, the reference turbine had the best efficiency over the widest TSR when the blade pitch angle was set to +4°. When the blade pitch angle was set to 0° the force

on the blade contributed more to the thrust, while for $+8^\circ$, the increased pitch angle resulted in a reduced angle of attack and hence lower thrust force on the turbine.

4.3 Effect of different leading-edge tubercle profiles

Following the tests with the reference turbine, the two counterpart turbines with the different leading-edge profiles were tested using the test matrix given in Table 3 but at a constant incoming velocity of 2 m/s. The reason for selecting 2 m/s incoming velocity was due to the negligible effect of the Reynolds number on the turbine efficiency as opposed to the considerable effect of the cavitation as discussed in Section 4.1 and 4.2. Therefore, in order to investigate the effect of leading-edge tubercles on the blade performance independent from the cavitation and blade pitch angle, the result of the tests at 2m/s was used for comparisons with the results of the reference turbine. Each set of tests was repeated three times and averaged to achieve the final result.

First of all the turbine models with 0° pitch angle were tested and the results are presented in Figure 13. The top two plots show the power coefficients (C_p) and the thrust coefficients ($C_t/10$) and the bottom two plots show the comparison of different leading-edge tubercle profiles against the reference turbine. It can be seen that the leading-edge tubercles can improve the performance of the turbine in the lower range of TSRs (0.5 to 2.5), where the turbine is suffering from stall. Under these conditions, a turbine with leading-edge tubercles can generate more force, which can be observed in both C_p and $C_t/10$. Around 40% more torque can be achieved due to the lead-edge tubercles. However, with the increase in TSR, the C_p values of the Ref turbine and Sin_2 turbine reach a maximum value of 0.43, at $TSR=3.5$, while the turbine Sin_8 reached its maximum with a small delay at $TSR=4$. At the higher end of TSRs, turbines Sin_2 and Sin_8 can generate around 15 to 20% more torque and around 4% less thrust with the influence caused by Sin_8 more obvious than that of Sin_2.

Following the 0° pitch angle tests, the pitch angle setting was increased to $+4^\circ$, which was the most efficient pitch angle setting for the reference turbine, and the tests were repeated. As shown in Figure 14, similar to the results with the 0° pitch angle, the leading-edge tubercles can contribute more torque at the lower end of the TSR range as well as thrust. A maximum of 30% more torque can be produced at $TSR=1.5$. Compared with Sin_2, the impact caused by Sin_8 is more obvious in both C_p and $C_t/10$. On the other hand, the effect of the leading-edge tubercles was smaller relative to that at 0° pitch angle. As noted, the leading-edge tubercles did not have any effect on the maximum C_p apart from shifting its TSR from 3.5 to 4.0.

Following the same procedure, the turbine models with 8° pitch angle were tested and results evaluated. According to Figure 15, as expected and in-line with the results of the previous test cases, the tubercles improved the performance over the lower TSR range and did not have any obvious impact on the maximum C_p . However, the leading edge tubercles significantly increased the thrust coefficient, $C_t/10$, with around a 10% increment caused by Sin_8. This indicated that the blades are generating higher force however this force contributes more to the thrust than the torque.

5 Conclusions

A set of tidal turbine models with and without leading tubercles on their blades have been tested in the Emerson Cavitation Tunnel for further understanding of their effects on the

hydrodynamic performance of the turbines. According to the test result, the following conclusions can be drawn:

1. The impact of the leading-edge tubercles is mainly on the lower range of TSRs (up to 2.5), while the blade is operating under stall conditions. Leading-edge tubercles can greatly enhance the force generated by the turbine blade, which can both result in a higher torque and also a higher thrust.
2. For the lower pitch angles, the improvement caused by the leading-edge tubercles is higher than the case for the higher pitch angle. It was also demonstrated that the biomimetic concept can help to improve the performance while the turbine is working under stall conditions. Turbines with leading edge tubercles will start at a lower current velocity.
3. The application of the leading edge tubercle concept does not compromise the maximum power coefficient value of the turbine but slightly shifts the distribution of this coefficient over the tip speed ratios tested, towards the higher range.

Acknowledgments

This research is funded by the School of Marine Science and Technology, Newcastle University and the China Scholarship Council. The financial support obtained from both establishments is gratefully acknowledged. The Authors would also like to thank all the team members in the Emerson Cavitation Tunnel for the help in testing and sharing their knowledge.

Reference

- Atlar, M., 2011. Recent upgrading of marine testing facilities at Newcastle University, AMT'11, the second international conference on advanced model measurement technology for the EU maritime industry, pp. 4-6.
- Bahaj, A.S., Batten, W.M.J., McCann, G., 2007. Experimental verifications of numerical predictions for the hydrodynamic performance of horizontal axis marine current turbines. *Renewable Energy* 32 (15), 2479-2490.
- Corsini, A., Delibra, G., Sheard, A.G., 2013. On the role of leading-edge bumps in the control of stall onset in axial fan blades. *Journal of Fluids Engineering-Transactions of the Asme* 135 (8), 081104-081104.
- Gruber, T., Murray, M.M., Fredriksson, D.W., 2011. Effect of humpback whale inspired tubercles on marine tidal turbine blades, ASME 2011 International Mechanical Engineering Congress and Exposition. American Society of Mechanical Engineers, pp. 851-857.
- Howle, L.E., Jan 24, 2009. Whalepower wenvor blade. Bellequant Engineering, PLLC.
- Johari, H., Henoeh, C., Custodio, D., Levshin, A., 2007. Effects of leading-edge protuberances on airfoil performance. *Aiaa Journal* 45 (11), 2634-2642.
- K. L. Hansen, R. M. Kelso, Dally, B.B., 2009. The effect of leading edge tubercle geometry on the performance of different airfoils, ExHFT-7, Krakow, Poland.
- Khan, M., Bhuyan, G., Iqbal, M., Quaicoe, J., 2009. Hydrokinetic energy conversion systems and assessment of horizontal and vertical axis turbines for river and tidal applications: A technology status review. *Applied Energy* 86 (10), 1823-1835.
- Miklosovic, D.S., Murray, M.M., Howle, L.E., 2007. Experimental evaluation of sinusoidal leading edges. *Journal of Aircraft* 44 (4), 1404-1408.
- Shi, W., Atlar, M., Norman, R., Aktas, B., Turkmen, S., 2015. Biomimetic improvement for a tidal turbine blade, EWTEC 2015, Nantes, France.
- Shi, W., Wang, D., Atlar, M., Seo, K.-c., 2013. Flow separation impacts on the hydrodynamic performance analysis of a marine current turbine using CFD. *Proceedings of the Institution of Mechanical Engineers, Part A: Journal of Power and Energy*.
- Stanway, M.J., 2008. Hydrodynamic effects of leading-edge tubercles on control surfaces and in flapping foil propulsion. Massachusetts Institute of Technology.
- Swanson, T., Isaac, K.M., 2011. Biologically Inspired Wing Leading Edge for Enhanced Wind Turbine and Aircraft Performance. AIAA.
- van Nierop, E., Alben, S., Brenner, M., 2008. How bumps on whale flippers delay stall: An aerodynamic model. *Physical Review Letters* 100 (5).

Wang, D., Atlar, M., Sampson, R., 2007. An experimental investigation on cavitation, noise, and slipstream characteristics of ocean stream turbines. *Proceedings of the Institution of Mechanical Engineers, Part A: Journal of Power and Energy* 221 (2), 219-231.

Weber, P.W., Howle, L.E., Murray, M.M., 2010. Lift, drag, and cavitation onset on rudders with leading-edge tubercles. *Marine Technology and Sname News* 47 (1), 27-36.

Yoon, H.S., Hung, P.A., Jung, J.H., Kim, M.C., 2011. Effect of the wavy leading edge on hydrodynamic characteristics for flow around low aspect ratio wing. *Computers & Fluids* 49 (1), 276-289.

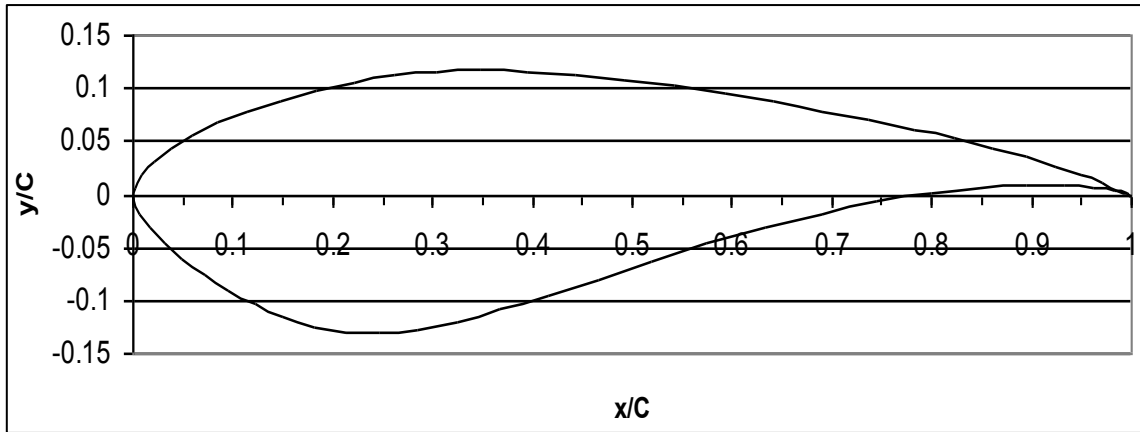


Figure 1 S814 foil section

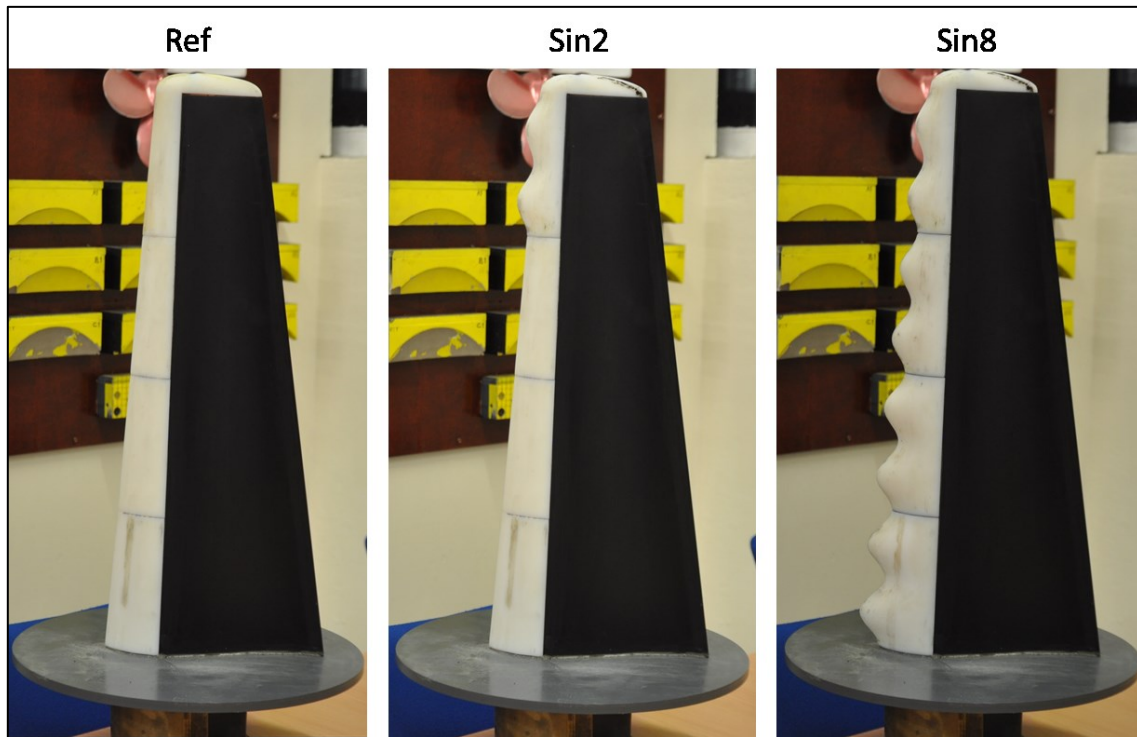


Figure 2 Hydrofoil models for the tubercle study (Shi et al., 2015)

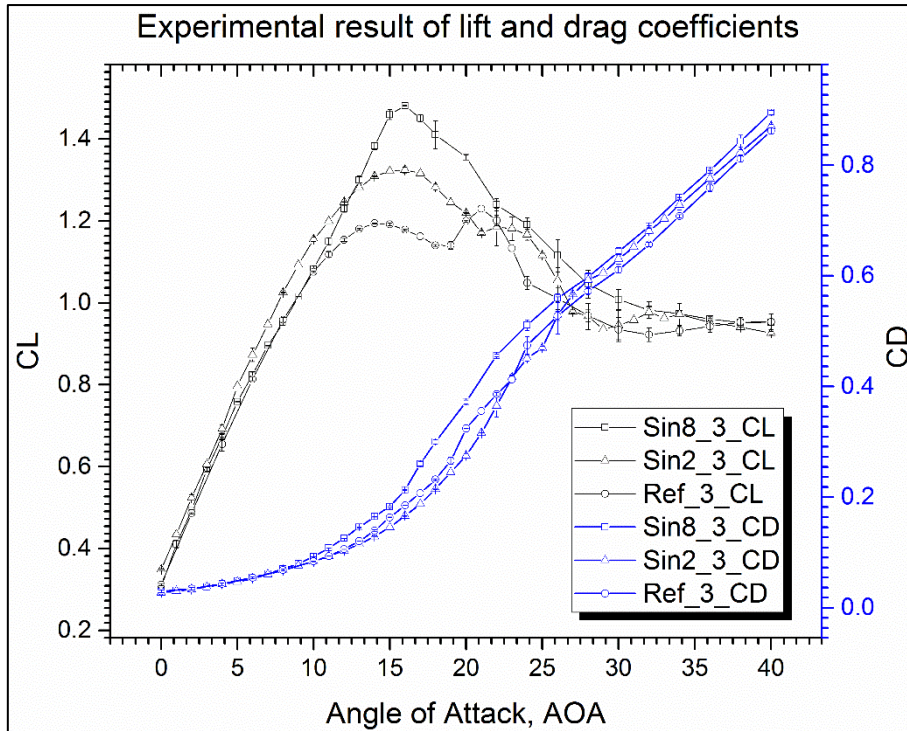


Figure 3 Lift and drag coefficients of the tested hydrofoils with different leading-edge design

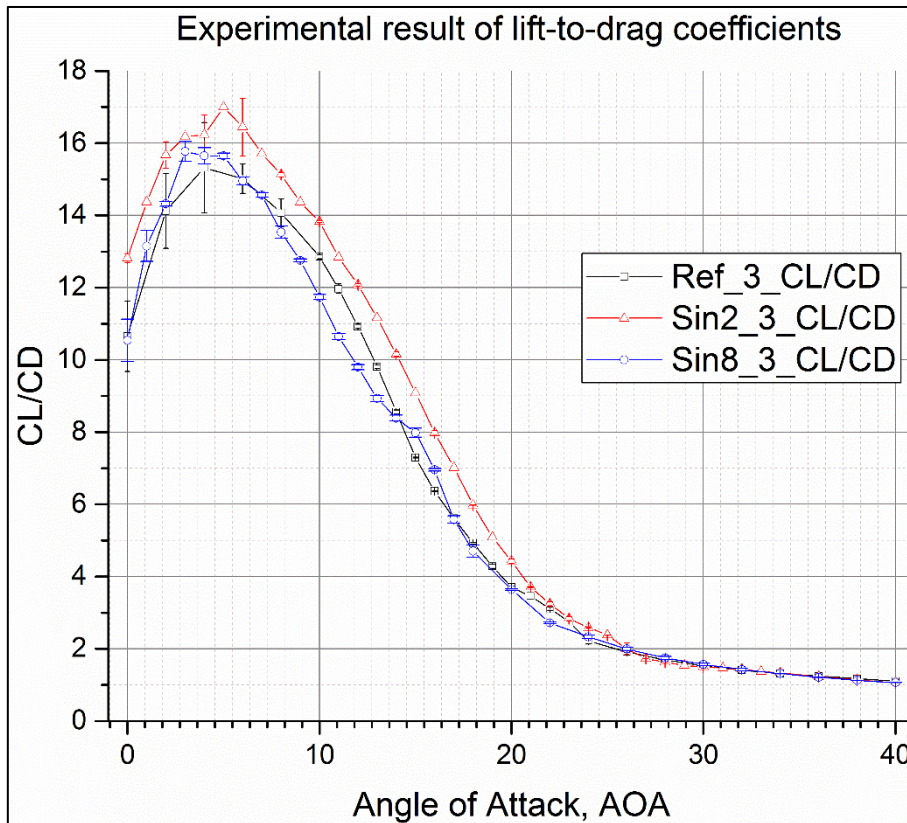


Figure 4 Lift-to-drag coefficients of the tested hydrofoils with different leading-edge design



Figure 5 Tested turbine models

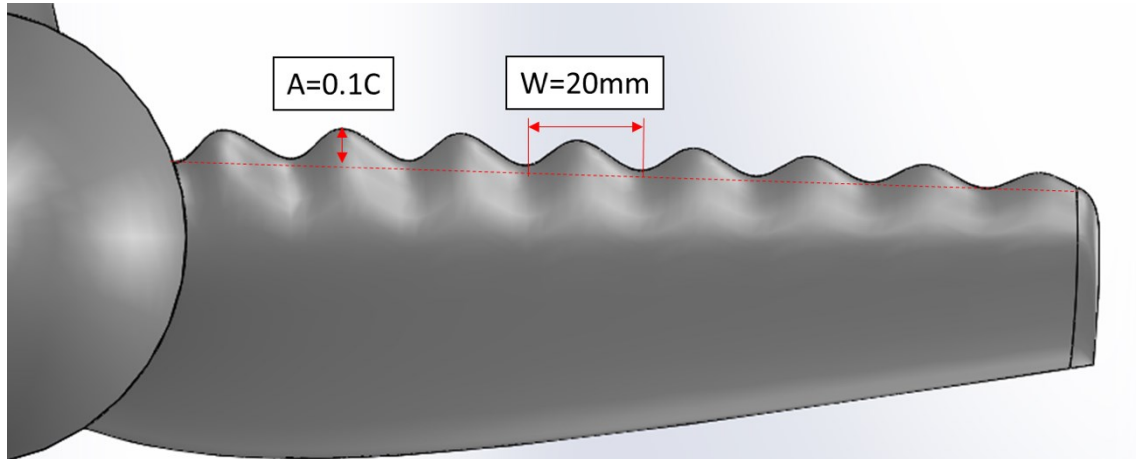


Figure 6 3D design of the turbine with leading-edge tubercles

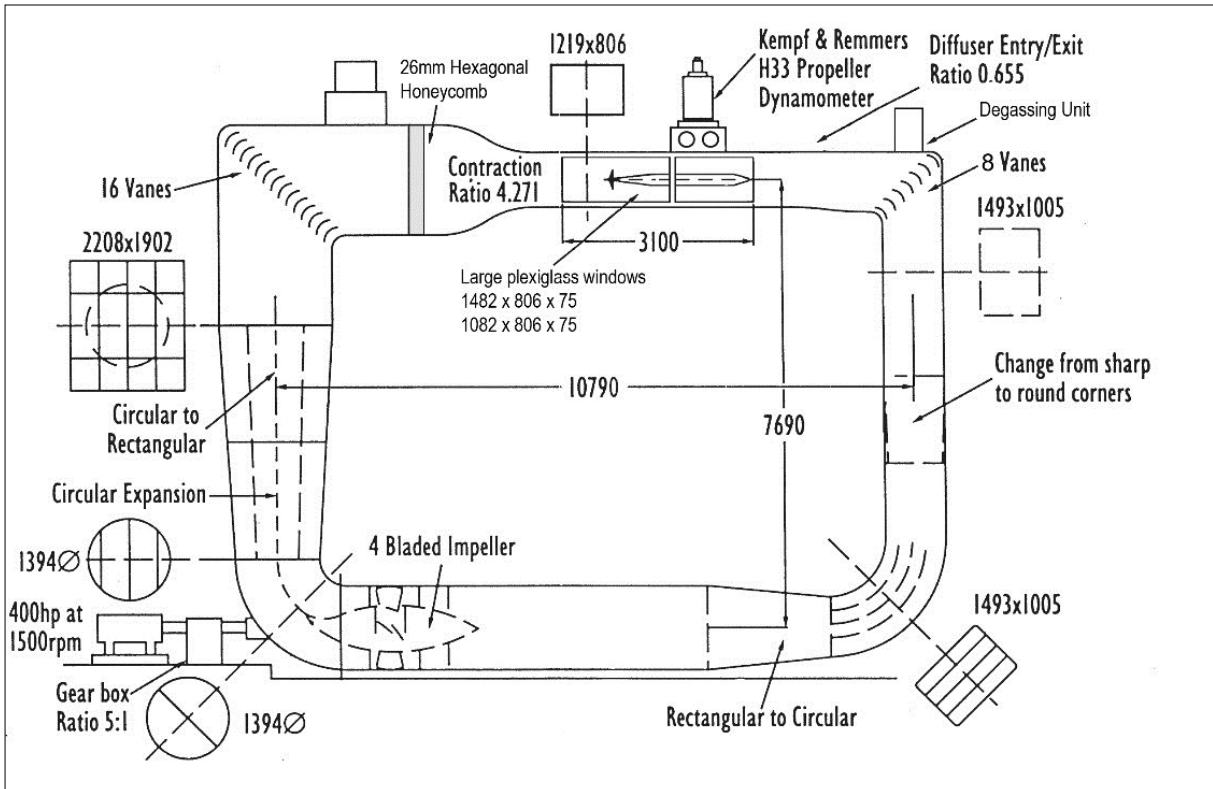


Figure 7 Sketch of ECT

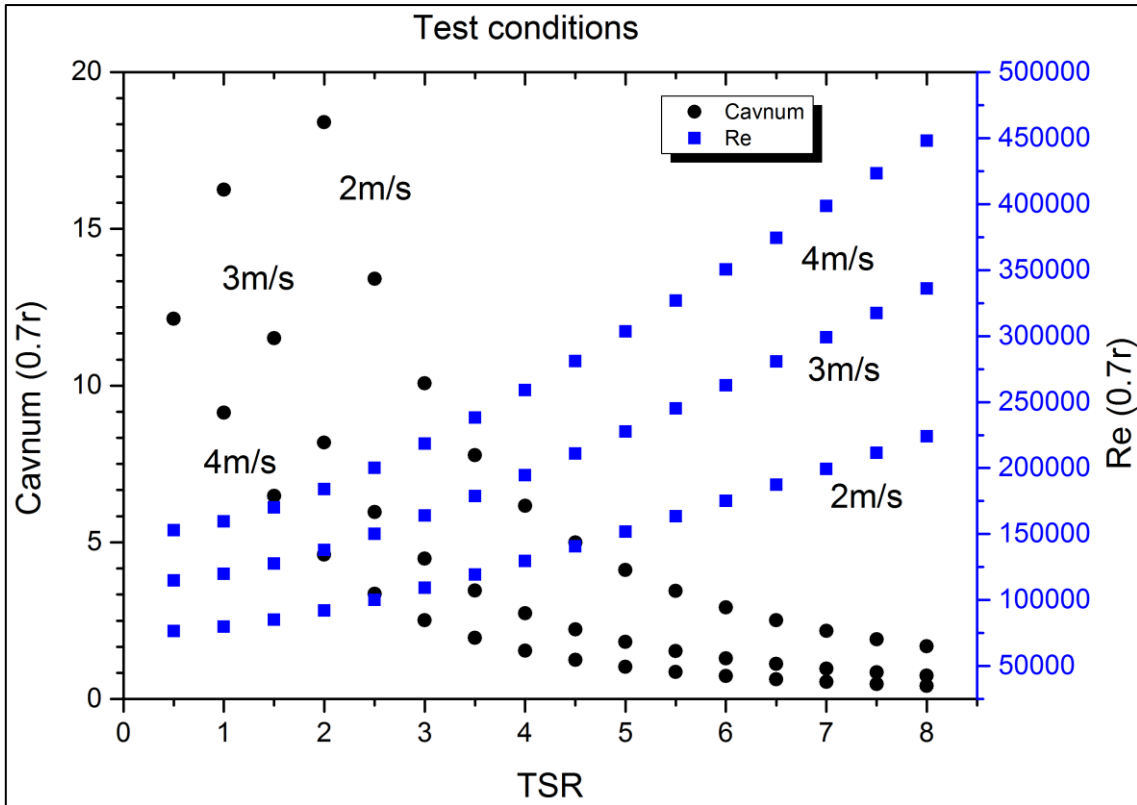


Figure 8 Test conditions

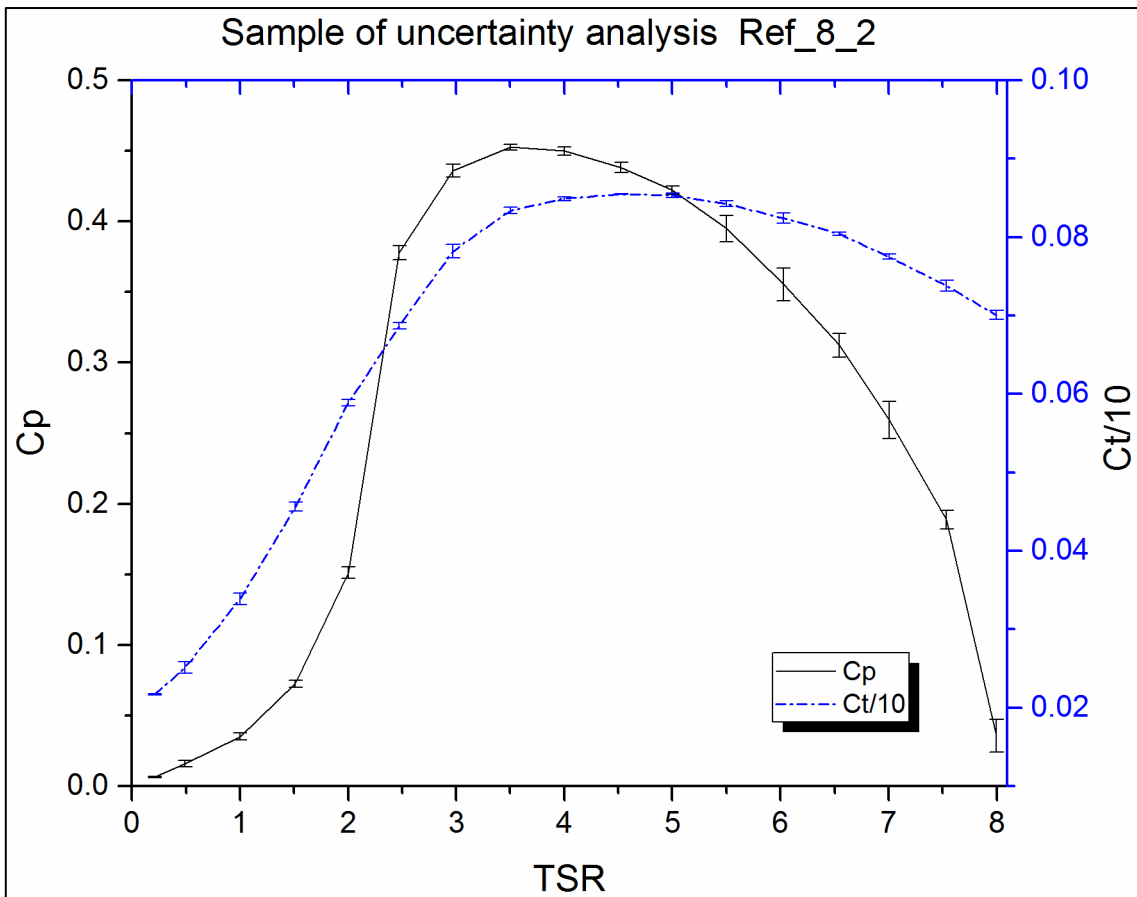


Figure 9 Sample of uncertainty analysis

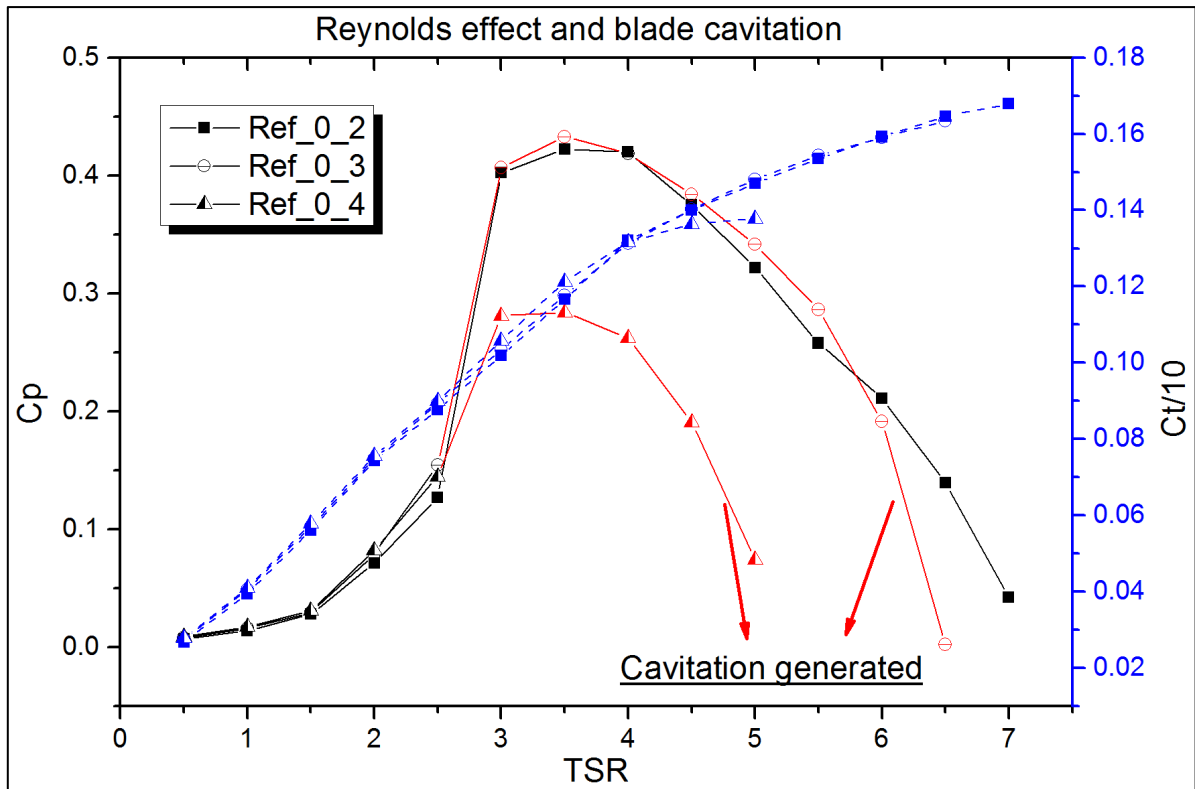


Figure 10 Influence on turbine performance caused by Reynolds number effect and blade cavitation

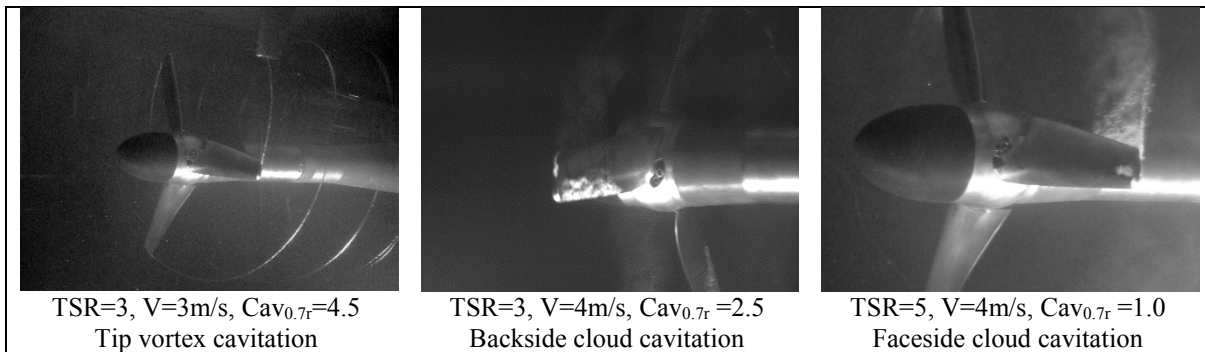


Figure 11 Types of blade cavitation

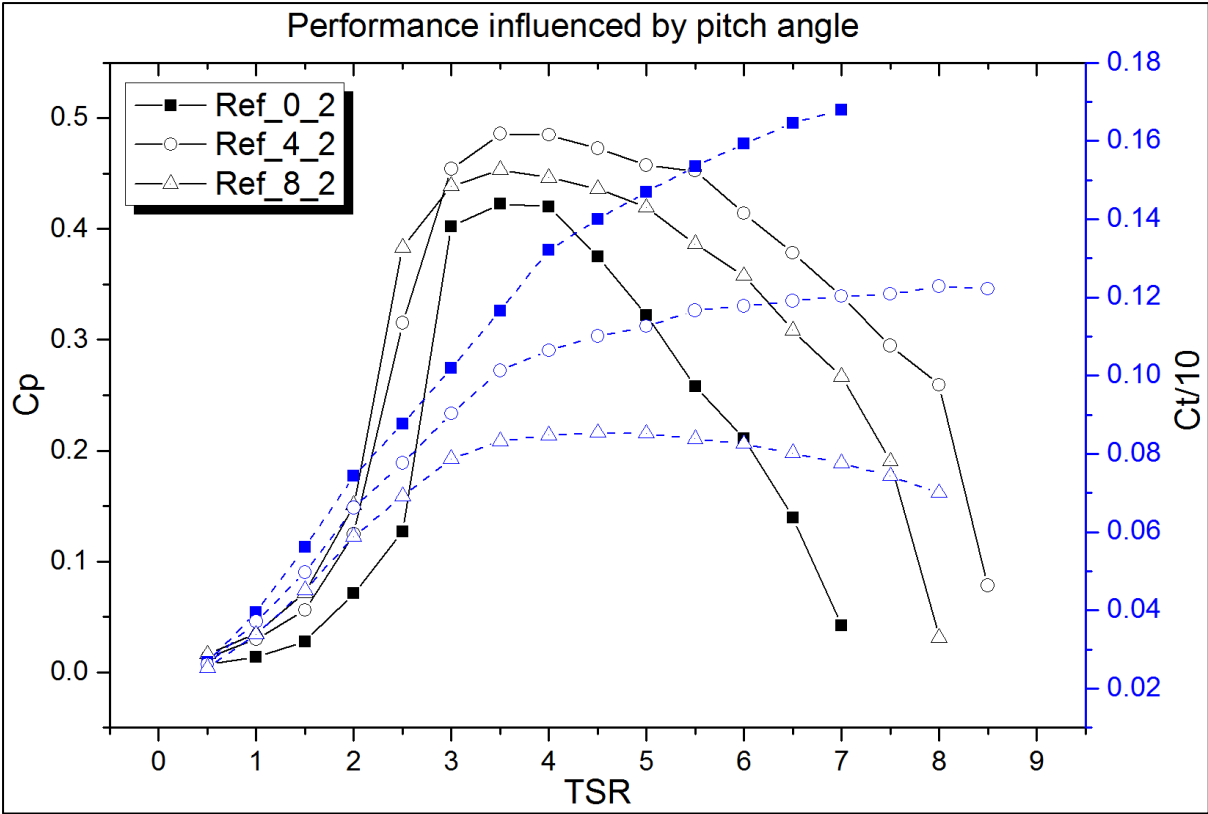


Figure 12 Performance influenced by pitch angle

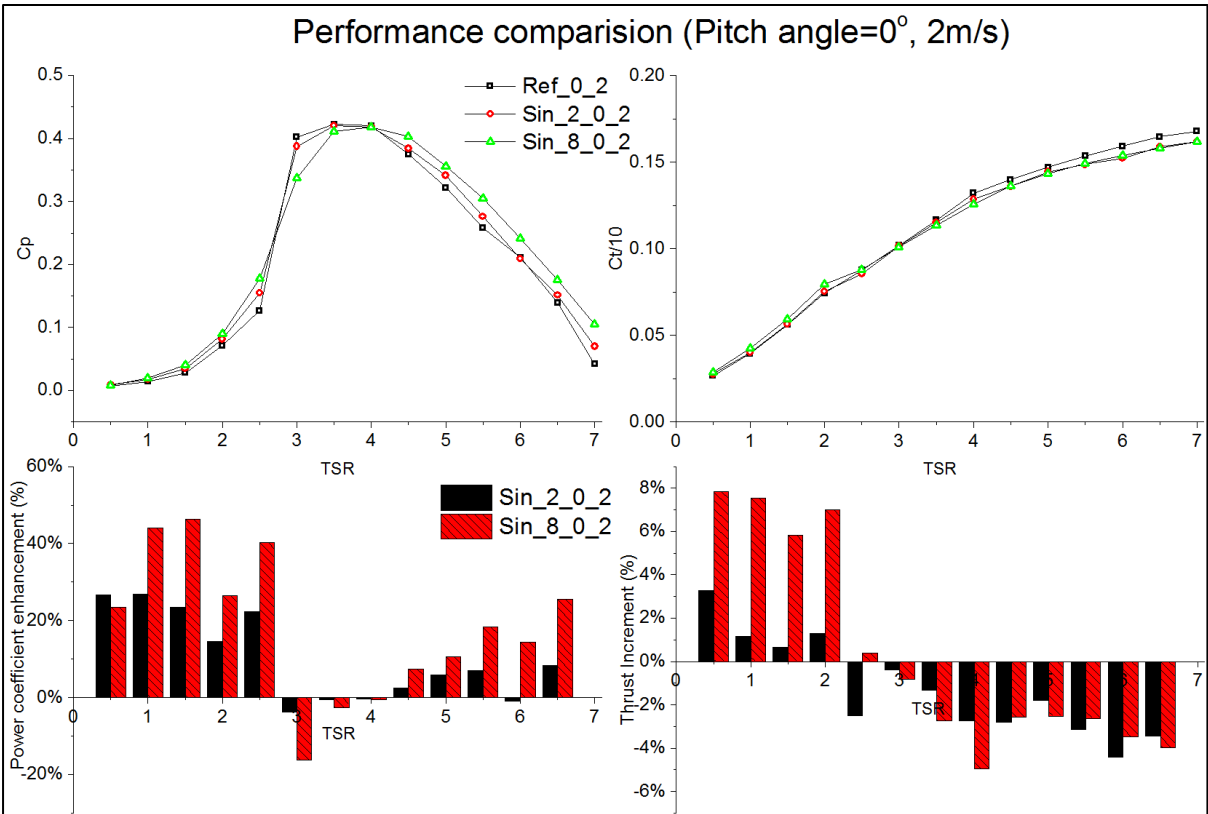


Figure 13 Performance comparison (Pitch=0°, 2m/s)

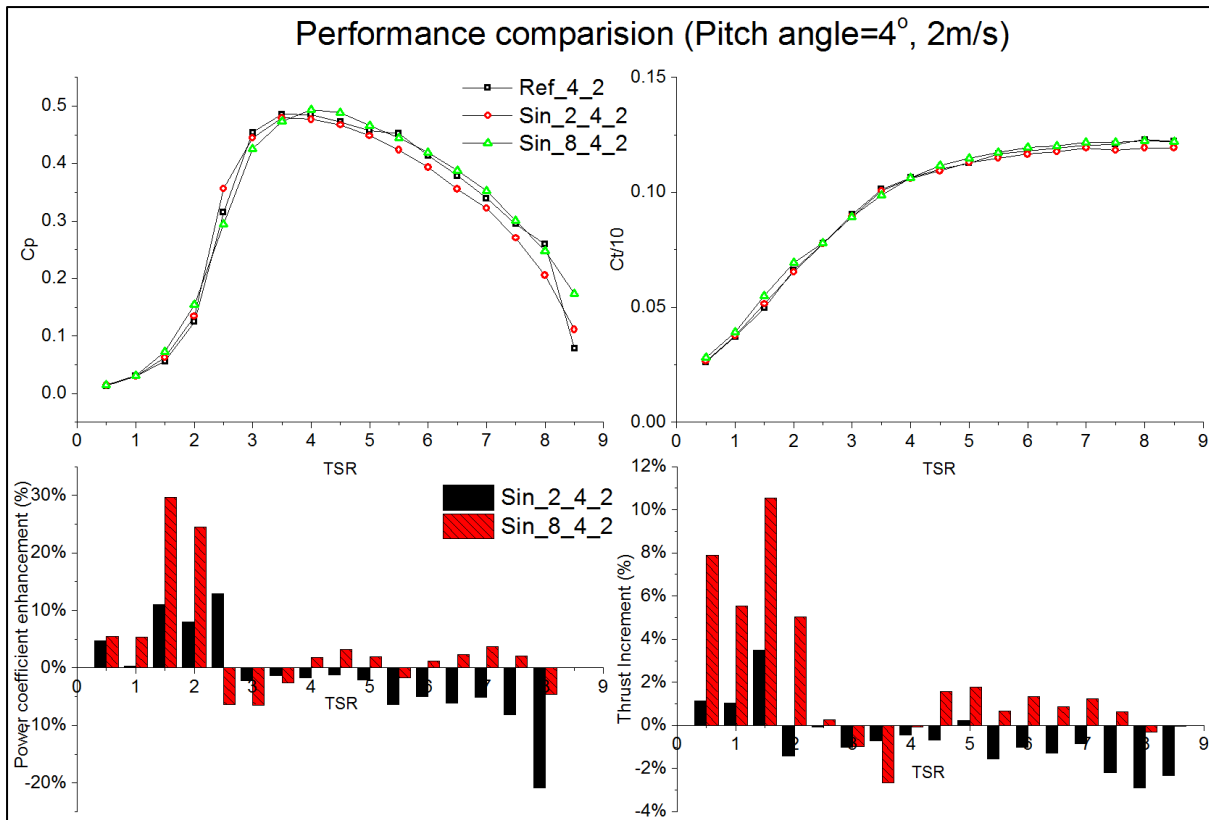


Figure 14 Performance comparison (Pitch=4°, 2m/s)

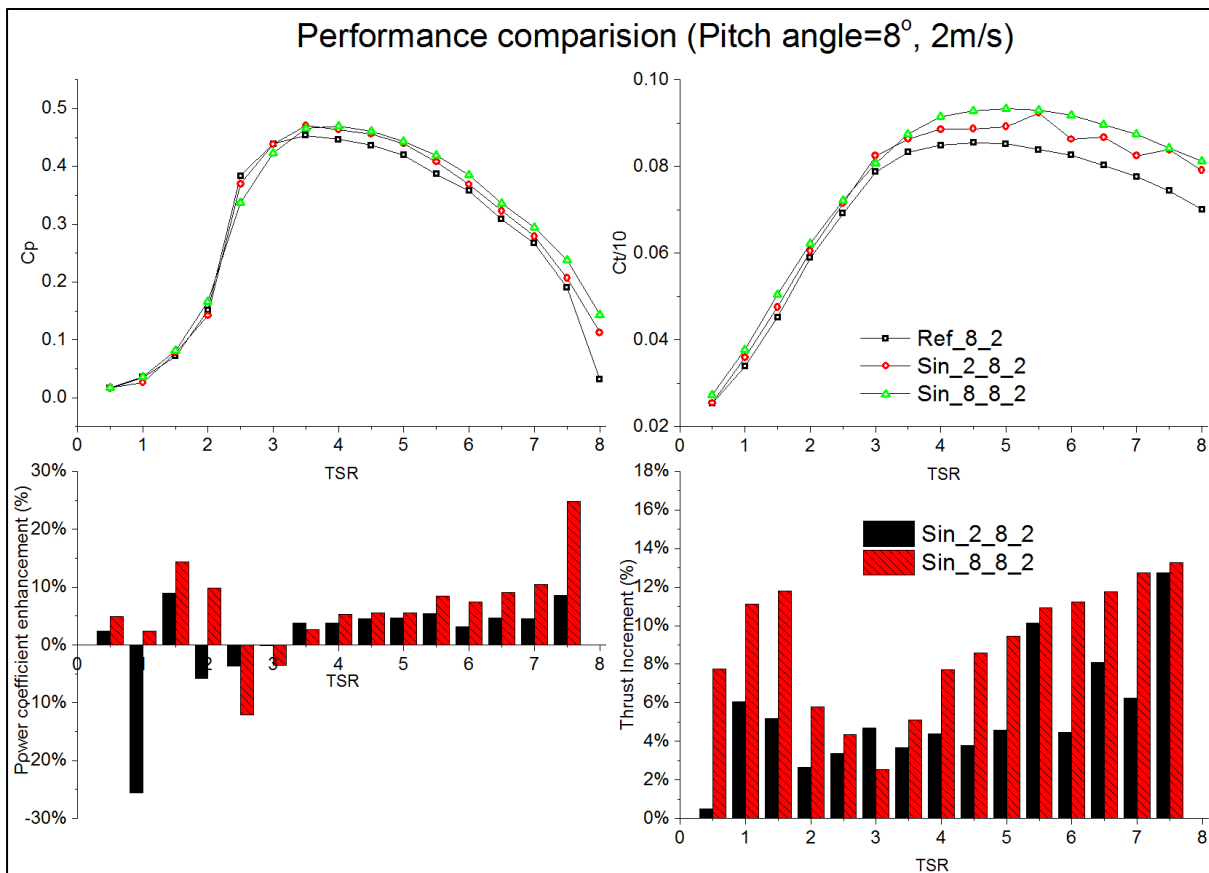


Figure 15 Performance comparison (Pitch=8°, 2m/s)

Table 1 Main particulars of the tidal stream turbine model

| | | | | | | | | | |
|-------------------|-------|-------|-------|-------|-------|-------|-------|-------|----|
| r/R | 0.2 | 0.3 | 0.4 | 0.5 | 0.6 | 0.7 | 0.8 | 0.9 | 1 |
| Chord length(mm) | 64.35 | 60.06 | 55.76 | 51.47 | 47.18 | 42.88 | 38.59 | 34.29 | 30 |
| Pitch angle (deg) | 27 | 15 | 7.5 | 4 | 2 | 0.5 | -0.4 | -1.3 | -2 |

Table 2 Technical data of propeller dynamometer H33

| | |
|------------------------------|---------------------|
| Type of dynamometer | Kempf & Rammers H33 |
| Rated maximum thrust (N) | ±3000 |
| Rated maximum torque (Nm) | ±150 |
| Maximum rotation speed (RPM) | 4000 |

Table 3 Test matrix

| V (m/s) | TSR | RPM | Pitch angle (°) | Tunnel pressure (mmhg) | Cav (0.7r) | Re (0.7r) |
|------------|---------|-----------|--------------------|---------------------------|----------------|---------------------|
| 2 | 0.5 ~ 8 | 47 ~ 763 | 0 | 850 | 48.534 ~ 1.684 | 0.76E+05 ~ 2.24E+05 |
| 2 | 0.5 ~ 8 | 47 ~ 763 | +4 | 850 | 48.534 ~ 1.684 | 0.76E+05 ~ 2.24E+05 |
| 2 | 0.5 ~ 8 | 47 ~ 763 | +8 | 850 | 48.534 ~ 1.684 | 0.76E+05 ~ 2.24E+05 |
| 3 | 0.5 ~ 8 | 71 ~ 1145 | 0 | 850 | 21.571 ~ 0.748 | 1.15E+05 ~ 3.36E+05 |
| 3 | 0.5 ~ 8 | 71 ~ 1145 | +4 | 850 | 21.571 ~ 0.748 | 1.15E+05 ~ 3.36E+05 |
| 3 | 0.5 ~ 8 | 71 ~ 1145 | +8 | 850 | 21.571 ~ 0.748 | 1.15E+05 ~ 3.36E+05 |
| 4 | 0.5 ~ 8 | 95 ~ 1527 | 0 | 850 | 12.134 ~ 0.421 | 1.53E+05 ~ 4.48E+05 |
| 4 | 0.5 ~ 8 | 95 ~ 1527 | +4 | 850 | 12.134 ~ 0.421 | 1.53E+05 ~ 4.48E+05 |
| 4 | 0.5 ~ 8 | 95 ~ 1527 | +8 | 850 | 12.134 ~ 0.421 | 1.53E+05 ~ 4.48E+05 |